

Automated Optimisation of Computationally Efficient Elastoplastic Winkler Model

S. K. Suryasentana, B. W. Byrne & H. J. Burd
University of Oxford, Oxford, UK

Abstract: This paper describes an automated approach for determining the optimal dimensions (length and diameter) of a suction caisson foundation subject to lateral loads, to minimise the foundation weight, whilst satisfying installation requirements, serviceability and ultimate limit states. The design problem was cast as a constrained optimisation problem. Solutions were initially developed using a graphical approach; the solution process was then repeated with an automated approach using an optimisation solver. Both approaches were feasible because a computationally efficient elastoplastic Winkler model was used to model the suction caisson foundation behavior under applied loading. The automated approach was found to be fast and reasonably accurate (when compared to more computationally expensive design procedures using three-dimensional finite element analyses). The benefits of this approach, made possible by the efficiency of the models employed, include better design outcomes and reduced design time.

Keywords: suction bucket, suction caisson, offshore engineering, finite-element, Winkler, optimisation

1 Introduction

1.1 Background

The design of a suction caisson foundation requires the satisfaction of three key limit states: fatigue limit state (FLS), serviceability limit state (SLS) and ultimate limit state (ULS). For simplicity, this paper considers only the SLS and ULS cases. The SLS condition requires the displacement and rotation of the foundation to be within certain limits, while the ULS condition requires that the design geotechnical and structural capacities of the foundation exceed the extreme design loads. For suction caisson foundations, the design must also satisfy installation requirements (i.e. whether the foundation can be installed with suction). The main objective of the design process is to find the most cost-effective design, while satisfying the above conditions. This process is usually iterative and involves the following processes:

1. Select an initial estimate of the foundation dimensions.
2. Compute the behaviour of the foundation under the design loads.
3. Check whether the computed foundation behaviour satisfies the limit states conditions and installation requirement.
4. If the conditions are satisfied but are overly conservative, try smaller dimensions. If the conditions are not satisfied, try larger dimensions
5. Evaluate the cost of the design
6. Iterate until the most cost-effective design that meets the conditions is obtained.

The above iterative process is usually done manually and is time consuming and labour intensive. This is particularly the case for offshore wind farms, where designs may be required for hundreds of suction caisson foundations. An alternative approach would be to automate this iterative process by casting it as a constrained optimisation problem. This follows similar work by Doherty & Lehane (2017, 2018), on monopile foundation design, where constrained optimisation was applied to the objective of minimising foundation design cost, subject to the constraints posed by the limit states conditions. Doherty & Lehane (2017, 2018) determined the optimal embedded length and diameter of the minimum weight monopile foundation that satisfies both ULS and SLS conditions. The study expedites the design process by using computationally efficient Winkler models based on lateral soil reactions (Suryasentana & Lehane 2014, 2016).

1.2 Elastoplastic Winkler model

In the current work, a novel elastoplastic Winkler model, termed ‘OxCaisson-LEPP’ is used to model the suction caisson foundation behavior. OxCaisson-LEPP combines linear elastic soil reactions (Suryasentana et al. 2017) with local plastic yield surfaces, which have been calibrated using three-dimensional (3D) finite element analyses. Compared to non-linear elastic Winkler models such as the p - y and t - z methods (API, 2010; DNV, 2014), this elastoplastic Winkler model offers significant advantages such as realistic modelling of phenomena such as hysteresis and the interaction of different local load and moment components at failure. The OxCaisson-LEPP model employed in this paper is similar to that described in Suryasentana et al. (2018), except that it has been calibrated for caissons of $0 \leq L/D \leq 2$ using the approach described in Suryasentana et al. (2019b). The soil model used to calibrate OxCaisson-LEPP is von Mises soil (representing undrained clay) with s_u profile assumed constant with depth.

A key advantage of using an elastoplastic Winkler model, compared to elastoplastic macro-element models (e.g. Cassidy 2004, Salciarini et al. 2011), is its generality. Given the localised nature of the soil reactions and the yield surfaces, the Winkler model can be adapted to non-homogeneous grounds with arbitrary yield strength profiles. This contrasts with macro-element models, which can only be adapted to ground profiles similar to that used in the calibration. In the current paper, this hypothesis is tested using a case study, in which the ground model is based on the Cowden stiff clay profile (which has a non-homogeneous s_u profile) used in the recent PISA project (Byrne et al. 2017).

1.3 Automated optimisation of suction caisson foundations

An example design case is described below in which optimal values of skirt length L and diameter D are determined automatically for a suction caisson foundation supporting an offshore wind turbine, by casting the design problem as a constrained optimisation problem. The optimisation problem was first solved using a graphical approach and then an automated approach using an optimisation solver. The design of a suction caisson foundation is strongly influenced by the installation process. To demonstrate this, two optimal designs have been obtained; one considering installation of the design and the other in which installation is not considered.

2 Methodology

2.1 Design case

The case study in this paper adopts, as an example, the design loads in Tab. 1 (Doherty & Lehane, 2017). These design loads relate to a 3.6 MW offshore wind turbine located in the London Array wind farm, in a water depth of approximately 25 m.

Tab. 1. Factored SLS and ULS design loads for the London Array wind farm (Doherty & Lehane 2017).

| | SLS | ULS |
|------------------------------------|---------|------------|
| Max lateral load at ground level | 5.33 MN | 7.20 MN |
| Max bending moment at ground level | 219 MNm | 295.65 MNm |

OxCaisson-LEPP is calibrated for undrained clay, so the current study adopts the Cowden clay profile used during the PISA project (Byrne et al. 2017), as a representative soil. The profiles of the small strain shear modulus G_0 and undrained shear strength s_u for the Cowden site – as employed in the current study - are illustrated in Fig. 1.

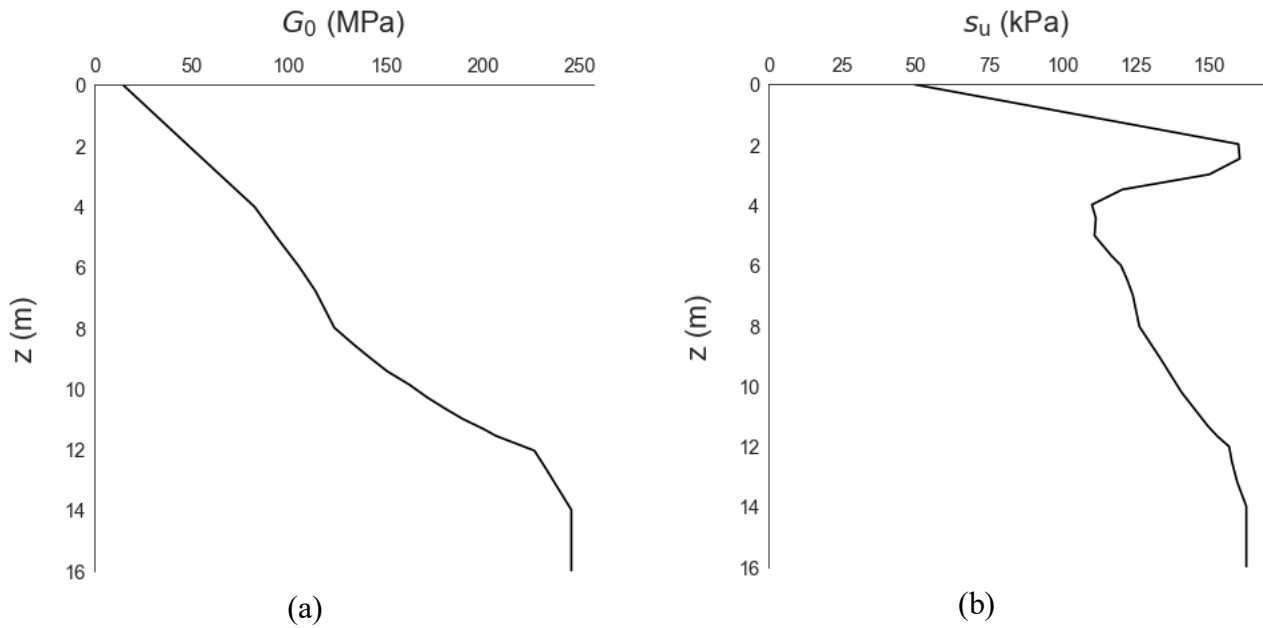


Fig. 1. Small strain shear modulus G_0 and undrained shear strength s_u profiles (Byrne et al., 2017) adopted for the current case study. The G_0 and s_u profiles are assumed to be uniform at depths below 14 m.

2.2 Design problem (without the installation constraint)

The objective of the design problem is to find the lowest cost foundation design that satisfies the limit state conditions. The foundation cost is assumed to be primarily determined by its material cost, which depends on its steel volume. For this study, the normalized wall thickness d_{skirt}/D is assumed to be 0.005 (following Houlsby et al., 2005), and the normalised lid thickness d_{lid}/D is assumed to be 0.05. Fig. 2 shows a schematic diagram of the suction caisson foundation.

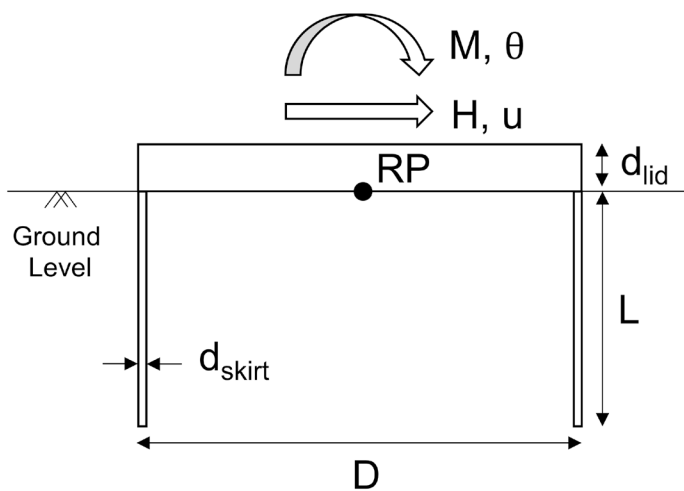


Fig. 2. Schematic diagram of a suction caisson foundation. RP is the loading reference point.

The steel volume of the caisson is:

$$\text{Vol}_{\text{caisson}} = \pi D^3 (0.004975 L/D + 0.0125) \quad (1)$$

The following SLS and ULS conditions were adopted in the study. For SLS, the rotation of the foundation at ground level θ_M cannot exceed 0.5° (DNV 2013). For ULS, the design loads in Tab. 1 cannot exceed the capacity of the foundation (structural capacities are not considered here; the caisson foundation is assumed to be linear elastic). This is defined in terms of a ‘distance to failure’ measure d_{ULS} , which measures how close the ULS design loads are to the global failure envelope of the foundation. Specifically, d_{ULS} is the magnitude of the ULS design loads, relative to the magnitude of its codirectional projection on the failure envelope (see Fig. 3 for an illustration of this).

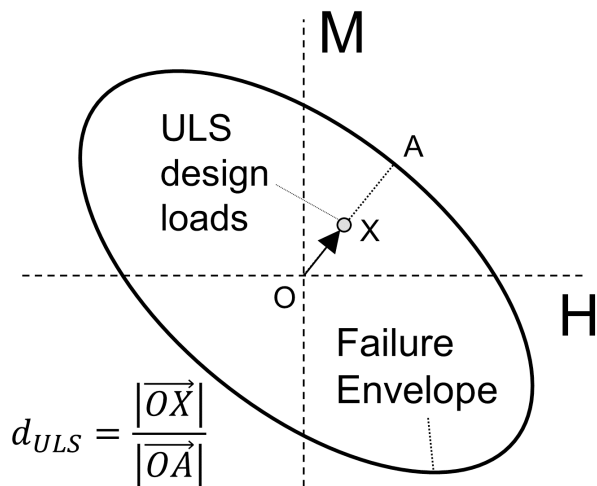


Fig. 3. d_{ULS} is the ratio of the magnitude of the ULS design loads to the magnitude of its codirectional projection on the global failure envelope (i.e. Point A in the figure). $d_{ULS} = 1$ means that the ULS design loads are on the failure envelope, while $d_{ULS} > 1$ means that the ULS design loads are outside the failure envelope.

Therefore, the design problem can be cast as the following optimisation problem:

$$\begin{aligned}
 &\text{minimise} && \text{Vol}_{\text{caisson}} && (2) \\
 &\text{subject to} && \theta_M \leq 0.5^\circ && \text{(SLS)} \\
 &&& d_{ULS} \leq 1 && \text{(ULS)}
 \end{aligned}$$

where the decision variables are D and L/D . OxCaisson-LEPP was used to compute θ_M and d_{ULS} , where the failure envelopes were computed using the sequential swipe test methodology as described in Suryasentana et al. (2019). Note that the sequential swipe test methodology is not exclusive to 3D finite element analyses and may be applied with elastoplastic Winkler models too.

2.3 Design problem (with installation constraint)

The design of a suction caisson foundation is heavily influenced by the installation processes. Since the water depth of this case study is assumed to be 25 m, the maximum suction pressure available before cavitation is approximately 350 kPa (this is a simplified estimate, as the actual value depends on factors such as the pump location etc.). Installation requirements thus impose an additional constraint on the design problem: the suction pressure p_{suction} required to install the caisson should not exceed 350 kPa. This design problem can be cast as the following optimisation problem:

$$\begin{aligned}
 &\text{minimise} && \text{Vol}_{\text{caisson}} && (3) \\
 &\text{subject to} && \theta_M \leq 0.5^\circ && \text{(SLS)} \\
 &&& d_{ULS} \leq 1 && \text{(ULS)} \\
 &&& p_{\text{suction}} \leq 350 \text{ kPa} && \text{(Installation)}
 \end{aligned}$$

where p_{suction} is computed using the procedures described by Houlsby & Byrne (2005), assuming a total vertical load of 3 MN and $\alpha_o = \alpha_i = 0.5$ during installation (α_o and α_i are adhesion factors on the outside and inside of the caisson, which are applied to the undrained shear strength to account for the interface response).

2.4 Solver

To solve Eqs. 2 and 3, the ‘fmincon’ solver in the optimisation toolbox of MATLAB was used. fmincon can find the minimum of an optimisation problem specified by:

$$\begin{aligned} &\text{minimise} && f(\mathbf{x}) && (4) \\ &\text{subject to} && \mathbf{c}(\mathbf{x}) \leq 0 \\ & && \mathbf{lb} \leq \mathbf{x} \leq \mathbf{ub} \end{aligned}$$

where $f(\mathbf{x})$ is the objective function, $\mathbf{c}(\mathbf{x})$ is the inequality constraints function, \mathbf{x} are the decision variables and \mathbf{lb} , \mathbf{ub} are the lower and upper bounds of the decision variables. To convert Eqs. 2 and 3 into the form of Eq. 4, the following are defined:

- $\mathbf{x} = [D, L/D]^T$
- $\mathbf{lb} = [6, 0]^T$
- $\mathbf{ub} = [18, 2]^T$
- $f(\mathbf{x}) = \pi D^3 (0.004975 L/D + 0.0125)$
- $\mathbf{c}(\mathbf{x}) = [\theta_M - 0.5^\circ, d_{ULS} - 1]^T$ (for Eq. 2) or $[\theta_M - 0.5^\circ, d_{ULS} - 1, p_{\text{suction}} - 350]^T$ (for Eq. 3)

fmincon requires an initial estimate of \mathbf{x} which was set to $[12, 1]^T$ (average of \mathbf{lb} and \mathbf{ub}).

3 Results

A graphical approach was first used to estimate the solution to the optimisation problem. The contours of d_{ULS} and θ_M were generated by interpolation from a set of computed data points corresponding to $D = 6, 8, 10, 12, 14, 16, 18$ and $L/D = 0, 0.25, 0.5, 1, 1.5, 2$. OxCaisson-LEPP took 14 and 7 minutes to compute the d_{ULS} and θ_M data points respectively.

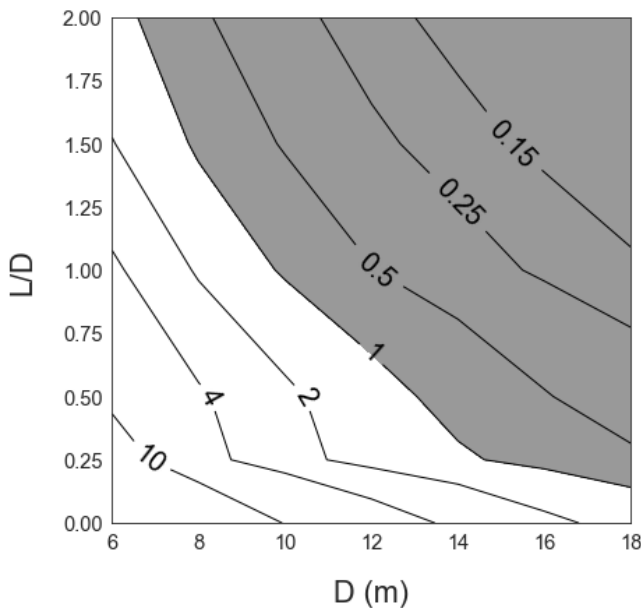


Fig. 4. Contour plots of d_{ULS} (value shown in contour label), as computed by OxCaisson-LEPP. The filled region represents the feasible combinations of D and L/D that satisfy the ULS constraint of $d_{ULS} \leq 1$.

Fig. 4 shows contours of d_{ULS} on a D vs L/D plot. The filled region shown in Fig. 3 indicates combinations of D and L/D that satisfy the ULS constraint of $d_{ULS} \leq 1$.

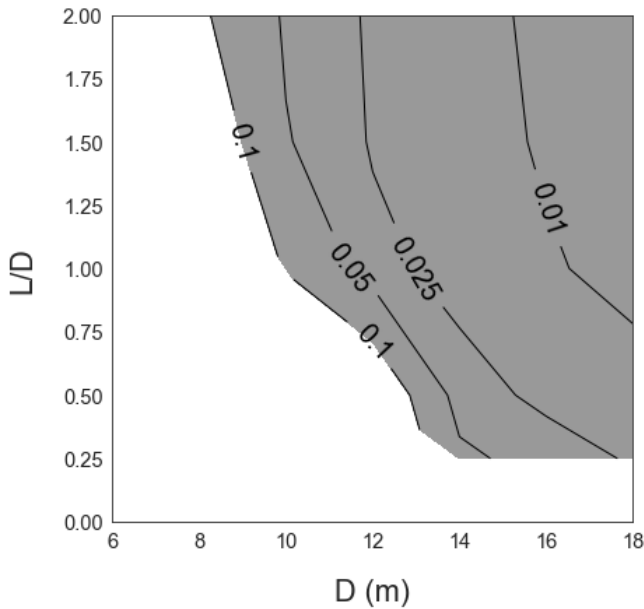


Fig. 5. Contour plots of θ_M (value shown in contour label) using OxCaisson-LEPP. The filled region represents the feasible combinations of D and L/D that satisfy the SLS constraint of $\theta_M \leq 0.5^\circ$. The unfilled region includes combinations of D and L/D where no solution can be obtained (as the SLS design loads exceed the capacity of the foundation). Note that there are no contours generated in the white region above, as there are no computations obtained in that area since the foundation capacity is reached at around $\theta_M = 0.1^\circ$.

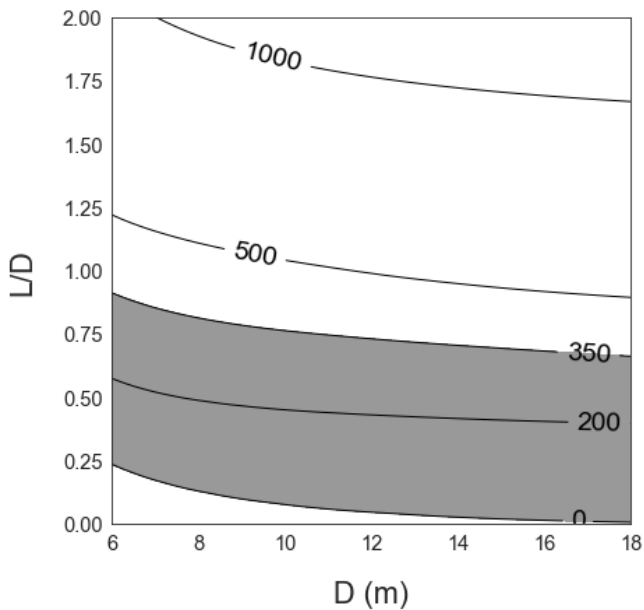


Fig. 6. Contour plots of the value of p_{suction} (in units of kPa) required to install the caisson. The filled region represents the feasible combinations of D and L/D that can be installed by suction, while the unfilled region below the filled region represents the combinations of D and L/D that can be installed by self-weight alone).

Figs. 5 and 6 plot the contours for θ_M and the suction pressure required for installation respectively, in terms of D and L/D . It is evident that suction installation limits the feasible dimensions of the caisson to low L/D ratios.

3.1 Graphical results

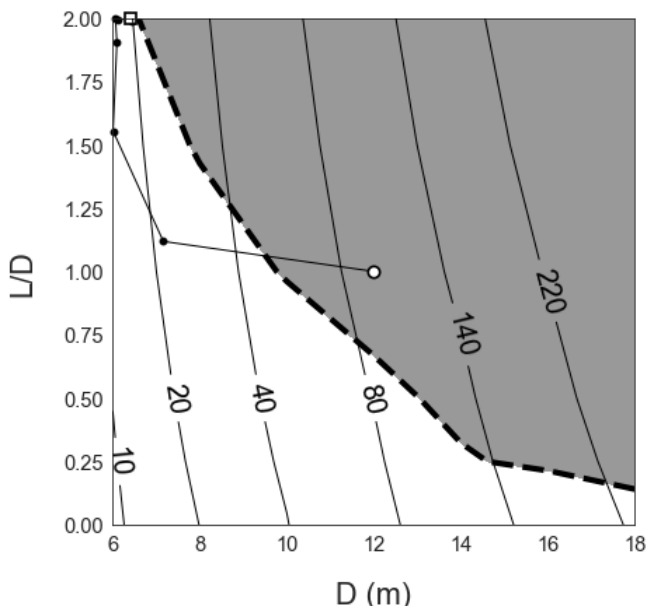


Fig. 7. Contour plots of the suction caisson steel volume (value shown in contour label in m^3 units). The thick black dashed lines represent the limiting ULS constraint. The limiting SLS constraint $\theta_M = 0.5^\circ$ is not showed in the figure as the foundation capacity is reached before reaching the SLS constraint. The filled region represents the feasible combinations of D and L/D that satisfy both the SLS and ULS constraints. The figure also indicates the progress of the optimisation problem solver, starting from the initial estimate (shown as the white circle marker) until the final, optimal result (shown as the white square marker).

Fig. 7 shows contours of the suction caisson steel volume (i.e. the objective function of Eq. 2) in terms of D and L/D . It is clear that the minimum volume lies in the region of low D and high L/D . This can be readily observed from Eq. 1, which shows that the suction caisson steel volume varies linearly with L/D , but cubically with D . Furthermore, the filled region in Fig. 7 represents the feasible combinations of D and L/D that satisfy both the SLS and ULS constraints. Based on the contours, the optimal dimensions is estimated to be the point at the top left corner of the feasible region, corresponding to $D = 6.7$ m, $L/D = 2$ and caisson steel volume = $21.2 m^3$.

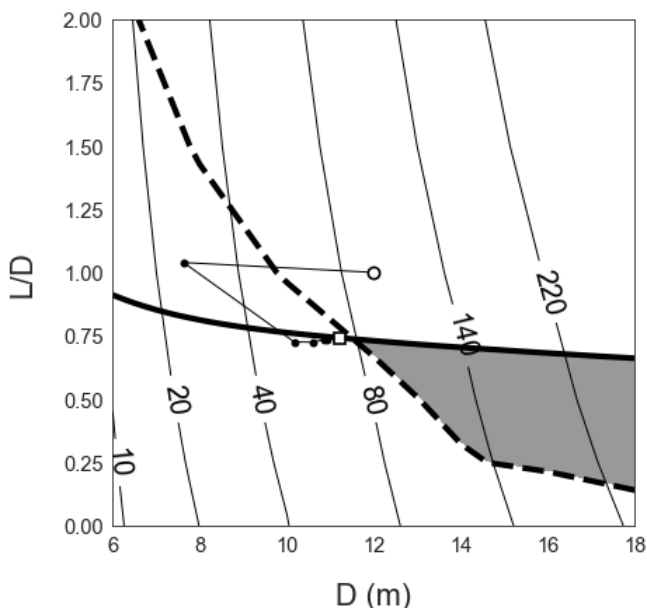


Fig. 8. Contours of suction caisson steel volume (in units of m^3). The thick black dashed and solid lines represent the ULS and installation constraints respectively. The filled region represents the feasible combinations of D and L/D that satisfy the SLS, ULS and installation constraints. The figure also indicates the progress of the optimisation problem solver, starting from the initial estimate (shown as the white circle marker) until the final, optimal result (shown as the white square marker).

Fig. 8 updates the data in Fig. 7, to include an additional installation constraint. The filled region represents the feasible combinations of D and L/D that satisfy the SLS, ULS and installation constraints. Compared to the results in Fig. 7, it can be observed that the feasible region is now restricted to caisson dimensions of low L/D and high D . Based on the contour plot in Fig. 8, the optimal dimensions is estimated to be the point at the top left corner of the feasible region, corresponding to $D = 11.4$ m, $L/D = 0.75$ and caisson steel volume = 75.5 m³.

3.2 Solver results

Figs. 7 and 8 show the progress of the optimisation problem solver, starting from the initial point ($D = 12$ m, $L/D = 1$) until the final, optimal points. The solver took about 11 trials for each problem. These optimal points are close to the values estimated by the graphical approach, as shown in Tab. 2. A better estimate can be obtained using the graphical approach by computing more data points for more accurate contours, but that would require more computational time.

Tab. 2. Optimal caisson dimensions based on the graphical and solver approaches

| Optimisation problem | Graphical | | | Solver | | |
|----------------------|-----------|-------|------------------------|---------|-------|------------------------|
| | D (m) | L/D | Vol. (m ³) | D (m) | L/D | Vol. (m ³) |
| Eq. 2 | 6.7 | 2 | 21.2 | 6.4 | 2 | 18.5 |
| Eq. 3 | 11.4 | 0.75 | 75.5 | 11.2 | 0.74 | 71.5 |

4 Discussion

It can be observed from Tab. 2 that the installation requirement means that the optimal steel volume is about 4 times that obtained without considering installation. Note that the analysis here is highly simplified, and a real design case needs to take into consideration structural fatigue behaviour for FLS, structural capacity for ULS and cyclic loading behaviour for SLS

The design problem could be solved quickly because OxCaisson-LEPP is very efficient. This would be impractical, if the 3D finite element method was used to compute the foundation response. For each optimization problem, the graphical and solver approaches took about 21 and 13 minutes respectively. One advantage of the graphical approach is that it allows a better understanding of the design problem through visualisation of the feasible parameter space, which is not possible with the solver approach. The main disadvantages of the graphical approach are: (i) the solution process is not automated (ii) the solution is not as accurate as the solver approach (iii) it is not suitable for optimisation problems with more than two decision variables.

For comparison purposes, a 3D finite element analysis of a suction caisson foundation with the optimal dimensions for Eq. 2 ($D = 6.4$ m, $L/D = 2$) in von Mises soil (using the G_0 and s_u profiles in Fig. 1) was carried out.

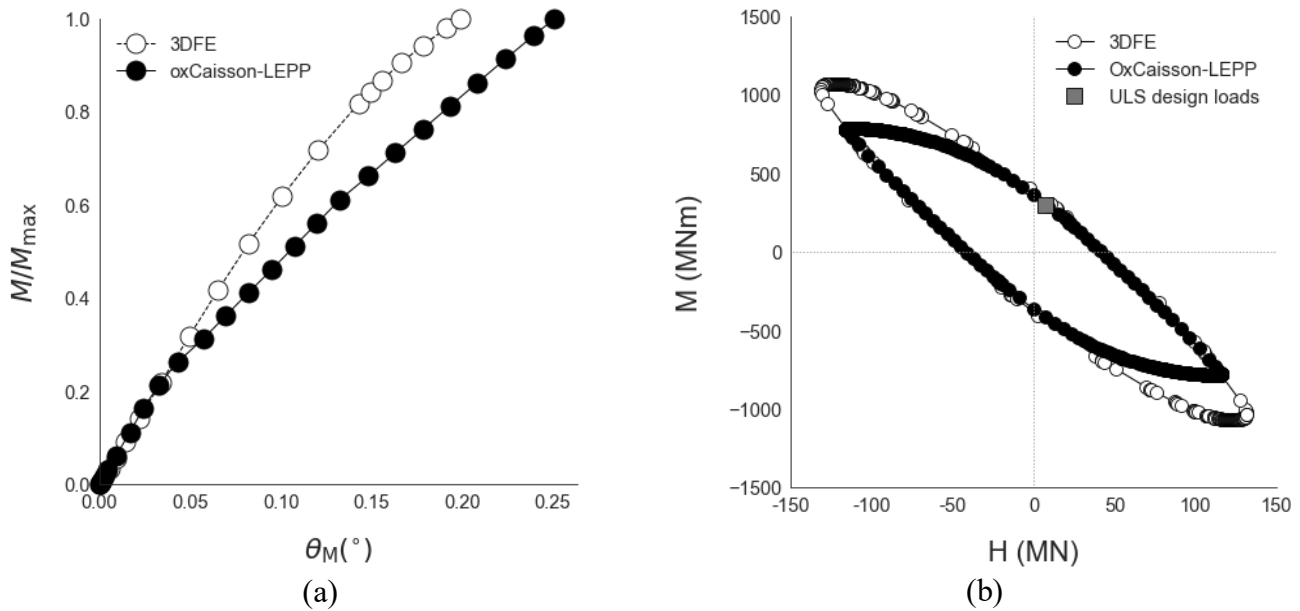


Fig. 9. Comparison of the OxCaisson-LEPP predictions with the 3D finite element results for (a) Ground level rotation θ_M of the foundation (b) Global HM failure envelope

Fig. 9a compares the OxCaisson-LEPP predictions of θ_M (under the SLS design loads) with the 3D finite element results. It is clear that the predicted θ_M agrees reasonably well with the 3DFE results and is less than 0.5° , thus satisfying the SLS constraint. Furthermore, global HM failure envelopes were obtained using the sequential swipe test (Suryasentana et al. 2019a). Fig. 9b compares the OxCaisson-LEPP predictions of the global HM failure envelope with the 3D finite element results. Again, the predictions agree well in the HM quadrants where H and M are of the same sign (most practical loading conditions), although the agreement is less in the other quadrants. Fig. 9b also shows that the ULS design loads are within the HM failure envelope, thus satisfying the ULS constraint.

There are some limitations with the current study. The automated foundation optimisation concept has only been applied to the Cowden Clay soil profile. Further work is required to investigate the applicability of this concept to other types of soil profiles (e.g. sand or non-homogeneous layered soil profiles).

5 Conclusion

This paper demonstrates the use of a computationally efficient model, OxCaisson-LEPP, to optimise the design of a suction caisson foundation for a practical case. OxCaisson-LEPP predictions were found to agree well with 3D finite element analyses. The efficiency of OxCaisson-LEPP allows the design of a suction caisson foundation to be automated and completed quickly. The automated design approach described in the paper was found to be very efficient; this not only reduces design time, but may also result in improved design outcomes. The proposed automated approach is particularly suitable for large-scale design exercises such as that for offshore wind farm foundations.

References

- API, 2010. RP 2A-WSD - Recommended Practice for Planning, Designing and Constructing Fixed Offshore Platforms. Washington: *American Petroleum Institute*
- Byrne, B. W., McAdam, R., Burd, H. J., Houlsby, G. T., Martin, C. M., Beuckelaers, W. J. A. P., Zdravkovic, L., Taborda, D. M. G., Potts, D. M., Jardine, R. J., Ushev, E., Liu, T., Abadias, D., Gavin, K., Igoe, D., Doherty, P., Skov Gretlund, J., Pacheco Andrade, M., Muir Wood, A., Schroeder, F. C., Turner, S. & Plummer, M. A. L., 2017. PISA: New Design Methods for Offshore Wind Turbine Monopiles, in *'Proceedings of the 8th International Conference for Offshore Site Investigation and Geotechnics'*, London.
- Cassidy, M. J., Martin, C. M. & Houlsby, G. T., 2004. Development and application of force resultant models describing jack-up foundation behaviour. *Marine Structures*, 17(3-4), pp.165-193.
- Doherty, J. P. & Lehane, B. M., 2017. An Automated Approach for Designing Monopiles Subjected to Lateral Loads, in *'Proceedings of 36th International Conference on Ocean, Offshore Arctic Engineering, OMAE 2017'*, Trondheim, Norway.
- Doherty, J. P., & Lehane, B. M., 2018. An automated approach for optimizing monopile foundations for offshore wind turbines for serviceability and ultimate limit states design. *Journal of Offshore Mechanics and Arctic Engineering*, 140(5), 051901.
- DNV, 2014. OS-J101 - Design of Offshore Wind Turbine Structures. Oslo: *Det Norske Veritas*.
- Houlsby, G. T., Kelly, R. B., Huxtable, J. & Byrne, B. W., 2005. 'Field trials of suction caissons in clay for offshore wind turbine foundations', *Géotechnique* 55(4), 287–296.
- Houlsby, G. T. and Byrne, B. W., 2005. Calculation procedures for installation of suction caissons in clay and other soils. *Proc ICE - Geotechnical Engineering* 158, No 2, pp 75-82.
- Salciarini, D., Bienen, B. & Tamagnini, C., 2011. A hypoplastic macroelement for shallow foundations subject to six-dimensional loading paths. *Proceedings of the 2nd international symposium on computational geomechanics (COMGEO-II)*, USA.
- Suryasentana, S. K. & Lehane, B. M., 2014. Numerical derivation of CPT-based p–y curves for piles in sand, *Géotechnique* 64(3), 186-194.
- Suryasentana, S. K. & Lehane, B. M., 2016. Updated CPT-based p–y formulation for laterally loaded piles in cohesionless soil under static loading. *Géotechnique* 66(6), 445-453.
- Suryasentana, S. K., Byrne, B. W., Burd, H. J., & Shonberg, A., 2017. Simplified Model for the Stiffness of Suction Caisson Foundations Under 6 DOF Loading. SUT OSIG 8th International Conference. London, UK.
- Suryasentana, S. K., Byrne, B. W. Burd, H. J., & Shonberg, A., 2018. An elastoplastic 1D Winkler model for suction caisson foundations under combined loading. *Proceedings of the 9th European Conference on Numerical Methods in Geotechnical Engineering (NUMGE 2018)*, Porto, Portugal.
- Suryasentana, S. K., Dunne, H., Martin, C., Burd, H. J., Byrne, B. W., & Shonberg, A., 2019a. Assessment of numerical procedures for determining shallow foundation failure envelopes. *Géotechnique (Ahead of Print)*.
- Suryasentana, S. K., Burd, H. J., Byrne, B. W. & Shonberg, A., 2019b. A Systematic Framework for Formulating Convex Failure Envelopes in Arbitrary Loading Dimensions. *Géotechnique (Ahead of Print)*.